

# NUSAP1 influences the DNA damage response by controlling BRCA1 protein levels

Shweta Kotian, Tapahsama Banerjee, Ainsley Lockhart, Kun Huang, Umit V Catalyurek, and Jeffrey D Parvin\*

Department of Biomedical Informatics; The Ohio State University Comprehensive Cancer Center; The Ohio State University; Columbus, OH USA

**Keywords:** NUSAP1, BRCA1, homologous recombination, centrosomes, DNA repair

**Abbreviations:** BRCA1, breast cancer associated gene 1; DDR, DNA damage response; DSB, DNA double strand break; HDR, homology directed repair; HR, homologous recombination; IRIF, ionizing radiation induced foci; NHEJ, non-homologous end joining; NUSAP1, nucleolar and spindle associated protein 1; SSA, single stranded annealing; 3'-UTR, 3'-untranslated region

NUSAP1 has been reported to function in mitotic spindle assembly, chromosome segregation, and regulation of cytokinesis. In this study, we find that NUSAP1 has hitherto unknown functions in the key BRCA1-regulated pathways of double strand DNA break repair and centrosome duplication. Both these pathways are important for maintenance of genomic stability, and any defects in these pathways can cause tumorigenesis. Depletion of NUSAP1 from cells led to the suppression of double strand DNA break repair via the homologous recombination and single-strand annealing pathways. The presence of NUSAP1 was also found to be important for the control of centrosome numbers. We have found evidence that NUSAP1 plays a role in these processes through regulation of BRCA1 protein levels, and BRCA1 overexpression from a plasmid mitigates the defective phenotypes seen upon NUSAP1 depletion. We found that after NUSAP1 depletion there is a decrease in BRCA1 recruitment to ionizing radiation-induced foci. Results from this study reveal a novel association between BRCA1 and NUSAP1 and suggests a mechanism whereby NUSAP1 is involved in carcinogenesis.

## Introduction

The breast cancer-associated gene 1 (*BRCA1*) is a well-documented breast and ovarian cancer specific tumor suppressor.<sup>1,2</sup> It is indispensable for a number of important biological functions including maintenance of genomic stability, transcription, and cell cycle checkpoint activation.<sup>3–6</sup> The BRCA1–BARD1 heterodimer co-localizes with  $\gamma$ -H2AX at DNA damage foci, recruiting other repair factors including RAD51 to the site of double strand breaks (DSBs).<sup>7,8</sup> In this manner, BRCA1 regulates a number of different repair processes, namely homologous recombination (HR), non-homologous end joining (NHEJ), and single strand annealing (SSA), and deficiency of BRCA1 severely impairs these processes.<sup>9–12</sup> The DNA damage response (DDR) is activated to repair DSBs by triggering cell cycle arrest, and marking cells for DNA repair by one of these processes.<sup>13,14</sup>

The nucleolar spindle-associated protein 1 (NUSAP1) is a gene encoding a 55 kD protein that is highly expressed in proliferating cells and interacts with microtubules.<sup>15</sup> Depletion of NUSAP1 caused faulty mitotic spindles, aberrant chromosome segregation, and defective cytokinesis. Overexpression of NUSAP1 caused microtubule bundling and cell cycle arrest at the G<sub>2</sub>/M checkpoint.<sup>16</sup> In response to DNA damage, NUSAP1 is phosphorylated by ATM/ATR kinases inducing a mitotic arrest,<sup>17,18</sup> and NUSAP1 has been shown to be degraded in response to UV damage.<sup>19</sup>

Numerous studies link elevated expression NUSAP1 to several cancers, including prostate, melanoma, glioblastoma, and hepatocellular carcinoma.<sup>20–24</sup> AML patients have higher levels of NUSAP1 antibodies in their serum.<sup>25</sup> NUSAP1 has been associated with increased disease aggression in meningiomas, poor prognosis and higher risk in breast cancers, and increased resistance to chemotherapy in pancreatic ductal adenocarcinoma patients.<sup>26–29</sup> NUSAP1 has also been identified as potential marker for breast ductal carcinoma in situ, and a cause of resistance.<sup>30</sup> Conversely, decreased NUSAP1 levels were seen in childhood ALL patients,<sup>31</sup> and the chromosomal locus associated with NUSAP1 is often deleted in cancers.<sup>19</sup>

Mutations of the highly penetrant *BRCA1* and *BRCA2* and of other genes, including *TP53*, *PTEN*, and *CHK2*, are responsible for ~30% of familial breast cancer;<sup>32,33</sup> we model that a substantial fraction of the missing ~70% of familial breast cancer is due to genes and gene combinations functioning in the same pathways as BRCA1/2. As a means to find candidates for the BRCA1/2 pathway proteins, we use gene co-expression networks.<sup>34</sup>

Based on initial computational analysis, we have identified *NUSAP1* expression to be strongly correlated with *BRCA1* expression in breast cancer microarrays. In this study, we have performed a biological validation of this finding. We found that NUSAP1 depletion impaired key functions that are also regulated by BRCA1, including homologous recombination and centrosome regulation. In addition, when BRCA1 was overexpressed, it

\*Correspondence to: Jeffrey D Parvin; Email: Jeffrey.Parvin@osumc.edu

Submitted: 10/10/2013; Revised: 01/13/2014; Accepted: 01/28/2014; Published Online: 02/12/2014  
http://dx.doi.org/10.4161/cbt.28019

rescued the defective phenotypes seen upon NUSAP1 depletion. This indicated that NUSAP1 and BRCA1 are implicated in the same pathways of DNA repair and centrosome duplication. Upon further investigation, we found that NUSAP1 controls BRCA1 protein abundance.

## Results

We performed a computational analysis of publicly available breast cancer microarray data sets to identify genes that are co-regulated with the reference genes *BRCA1*, *BRCA2*, and *BARD1*,<sup>34-36</sup> and also a novel two-step query-based biclustering approach, called correlated patterns biclusters (CPB).<sup>37,38</sup> This analysis finds genes with changes in mRNA abundance that match the reference genes in the many microarray samples. This approach allows one to utilize publicly available microarray results in order to find candidates for proteins that functionally interact with the reference genes/proteins. *NUSAP1* was one of the top-ranked genes that were co-expressed with these three reference genes across multiple data sets and multiple analytic methods (data not shown). *NUSAP1* was also found to be in a cell cycle and DNA repair network identified in a separate study.<sup>35</sup> The three reference genes/proteins are known to play a role in DSB repair and in the regulation of the centrosome duplication cycle. It was our hypothesis that *NUSAP1* would be important in these processes as well. Therefore, the role of *NUSAP1* in these processes was evaluated using the following tissue culture-based assays: homology-directed repair (HDR), DNA break repair by single strand annealing, and centrosome duplication.

### **NUSAP1 is required for full homologous recombination activity**

The HDR strategy is based on a recombination substrate that has been previously described.<sup>39</sup> The HeLa-DR cell line contains a single copy of this recombination substrate stably integrated in the genome, which encodes two inactive GFP alleles.<sup>40</sup> One of these alleles contains a specific 18 base pair I-SceI restriction endonuclease site. When these cells are transfected with a vector expressing the I-SceI enzyme, it generates a double strand break at the specific site. If in a given cell homologous recombination repairs the DSB, using homologous sequences in the second defective allele, then the recombination event converts the GFP gene to be active. The number of green fluorescent cells resulting from successful homologous recombination is measured using flow cytometry.

We tested the role of *NUSAP1* in homologous recombination by RNAi-mediated depletion in the HeLa-DR cell line. We found that *NUSAP1* depletion using any of three different siRNAs significantly decreased homologous recombination levels relative to the control (Fig. 1A). *NUSAP1* siRNA-2 and siRNA-4 had the strongest effect, reducing homologous recombination levels 2-fold. As all three siRNAs tested decreased homologous recombination, this effect was not due to off-target effects. All three *NUSAP1*-specific siRNAs efficiently depleted *NUSAP1* protein by immunoblot analysis (Fig. 1B). We prepared a *NUSAP1* expression plasmid that is resistant to one of the siRNAs, and co-transfection of this plasmid with the *NUSAP1*-specific siRNA

restored to nearly full extent the homologous recombination activity (Fig. 1C). The level of expression of the rescue protein was low, seen as the slowest migrating band in the immunoblot (Fig. 1D, lane 4), and perhaps this low level of re-expression was responsible for the incomplete rescue of homologous recombination.

We tested whether the effect of *NUSAP1* depletion on homologous repair was secondary to a cell cycle defect. We depleted *NUSAP1*, using two different siRNAs, in the HeLa-DR cell line, following the same protocol, and timeline as the HDR assay. Cells were harvested at 24, 48, and 72 h post second transfection, for measuring cell cycle progression using flow cytometry. Treatment with neither *NUSAP1* siRNA produced any significant changes in the cell cycle progression (Fig. S1).

### **NUSAP1 is required for DSB repair by single strand annealing**

We tested the effect of *NUSAP1* depletion on the process of DSB repair by single strand annealing (SSA) using another stable, recombinant HeLa cell line containing integrated in its genome a recombination substrate specific for the SSA pathway.<sup>11,41,42</sup> This cell line contains a GFP reporter system that is analogous to that of the HeLa-DR cell line, except significant resection is needed to expose sections of homology that can anneal to bridge the gap, resulting in a 2.7 kb deletion that converts the cell to GFP-positive. Upon depletion of *NUSAP1* in the SSA cell line, we found that transfection of siRNAs specific for *NUSAP1* inhibited the single strand annealing process by 30–50% (Fig. 1C). The magnitude of the deficit in DNA repair activity in *NUSAP1*-depleted cells was never as great as observed in *BRCA1*-depleted cells, but the decrease was statistically significant.

### **NUSAP1 depletion leads to formation of supernumerary centrosomes**

As it is known that depletion of *BRCA1* in mammary tumor cell lines causes centrosome amplification,<sup>43-45</sup> we investigated whether *NUSAP1* depletion would similarly result in centrosome amplification. *NUSAP1* siRNA was co-transfected along with a plasmid expressing GFP-tagged centrin,<sup>46,47</sup> into Hs578T breast cancer cells. GFP-centrin localized to the centrioles, which was visualized by fluorescence microscopy. In control siRNA treated cells, 4.5% of the cells had supernumerary centrosomes, whereas *NUSAP1* depletion resulted in 16% of cells with supernumerary centrosomes (Fig. 2; Fig. S2). A similar phenotype with centrosome amplification in 16% of cells was observed after *BRCA1* depletion, consistent with prior observations.<sup>43</sup> Transfection of two other siRNAs targeting *NUSAP1* similarly resulted in cells with multiple centrosomes (data not shown), indicating that this phenotype was not an off-target effect of the siRNA. Depletion of *NUSAP1* protein by these siRNAs was confirmed in the Hs578T cell line by immunoblot analysis (Fig. S3).

### **NUSAP1 was expressed during S/G<sub>2</sub> phases of the cell cycle**

Studies have shown that *NUSAP1* and *BRCA1* are expressed at similar stages in the cell cycle. *NUSAP1* levels increase as cells progress through S phase, peaking around the G<sub>2</sub>/M transition, and promptly decreasing in G<sub>1</sub>.<sup>15</sup> *BRCA1* levels increase through S phase, peaking at late S/early G<sub>2</sub> in the cell cycle.<sup>36,48</sup> We sought to directly compare *NUSAP1* with *BRCA1* cell cycle dependent

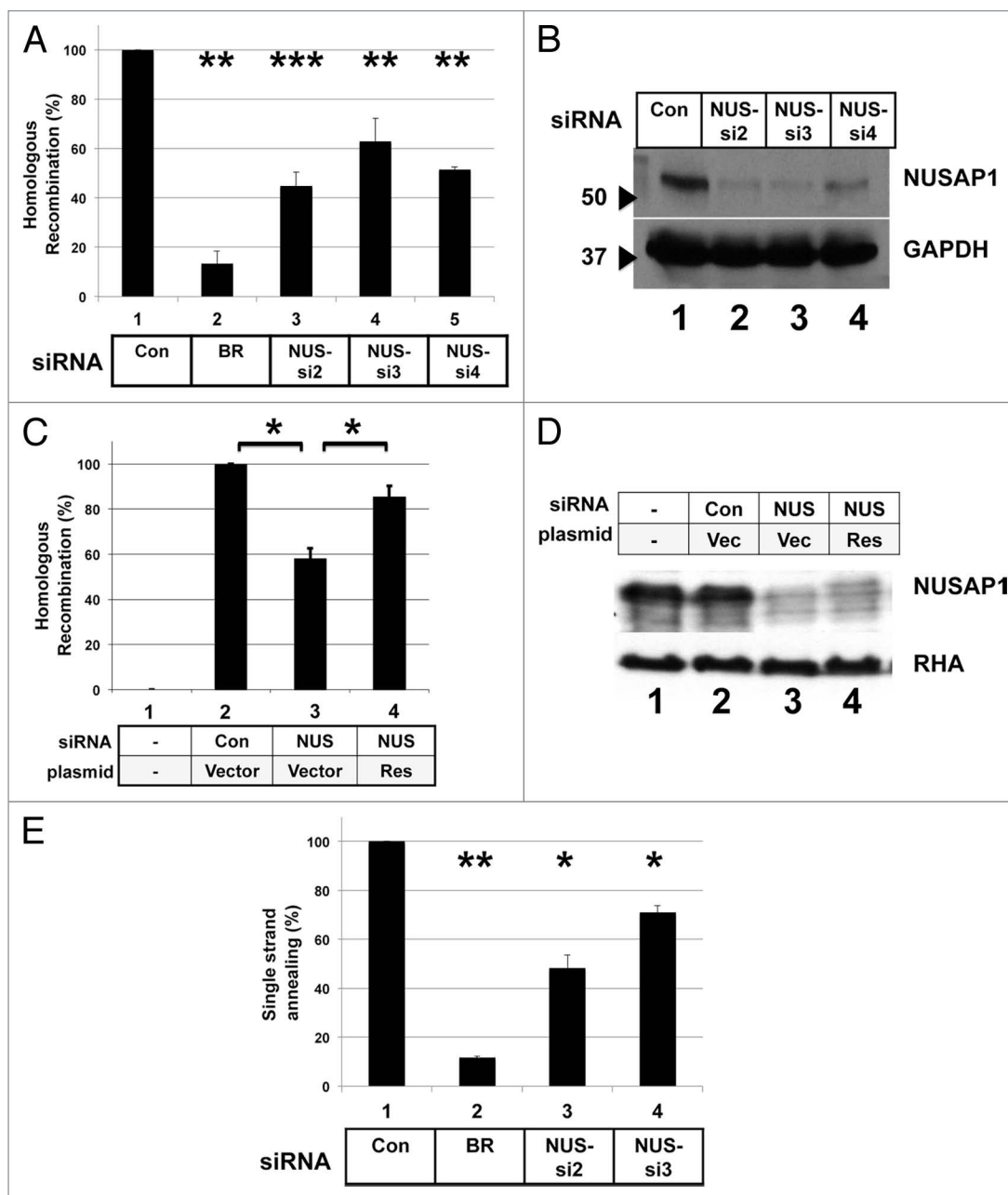


**Figure 1.** NUSAP1 is required for high levels of DSB repair by homologous recombination. **(A)** HeLa-DR cells, which contain integrated in the genome a recombination substrate for assaying HDR, were transfected with the indicated siRNAs, and then 2 d later transfected with the same siRNA plus a plasmid for the expression of the I-SceI endonuclease. Results were obtained in triplicate and normalized relative to the control (Con) siRNA with SEM. BRCA1 (BR) and NUSAP1 (NUS) siRNAs are indicated. A two-tailed Student *t* test was done for the NUSAP1 siRNAs compared with the control siRNA; *P* values for comparisons to the control siRNA were: 0.004195 for BRCA1; 0.0003138 for NUS-si2; 0.002255 for NUS-si3; and 0.002923 for NUS-si4. **(B)** Whole cell lysates were prepared from the leftover cells after assaying for HDR activity and analyzed by immunoblotting for antibody specific for NUSAP1 (top) and GAPDH as loading control (bottom). **(C)** HDR assay was done for HeLa-DR cells that were not transfected with I-SceI expressing plasmid (lane 1) or transfected with the following siRNAs and plasmids along with the I-SceI expressing plasmid: control siRNA and empty plasmid vector (lane 2); NUS-si2 and empty plasmid vector (lane 3); and NUS-si2 plus a plasmid encoding NUSAP1 with a conservative point mutation that renders the mRNA resistant to the siRNA (Res, lane 4). A two-tailed Student *t* test was done for NUSAP1 siRNA vs. control siRNA (lane 3 vs. lane 2; *P* = 0.02289) and NUS-si2 plus rescue transfection vs. NUS-si2 plus vector only (lane 4 vs. lane 3; *P* = 0.023224). **(D)** Samples from **(C)** were analyzed by immunoblotting with antibody specific to NUSAP1 (top) and RNA helicase A (RHA, bottom) as loading control. **(E)** HeLa-SA cells, which contain integrated in the genome a substrate that specifically measures recombination via the SSA pathway, were transfected with the indicated siRNAs. Results, in triplicate, were normalized to the control siRNA. A two-tailed Student *t* test was done comparing to the control siRNA; *P* values were: 0.006797 for BRCA1; 0.01224 for NUS-si2; and 0.02585 for NUS-si3.

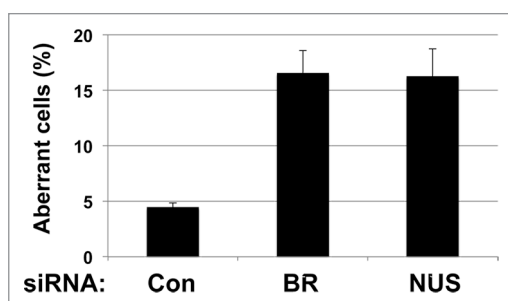


**Figure 2.** Depletion of NUSAP1 from Hs578T breast cancer cells results in supernumerary centrosomes. Hs578T cells were transfected with the indicated siRNA and a plasmid that expressed GFP-centrin2.<sup>47</sup> Centrosomes were counted in over 100 cells in each sample. Results, in triplicate, were normalized to the control siRNA.

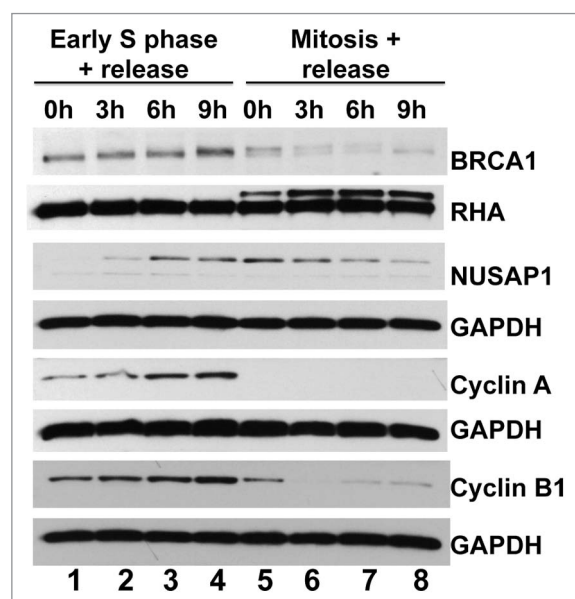


**Figure 3.** NUSAP1 protein expression occurs in S/G<sub>2</sub> phases of the cell cycle. HeLa cells were double-thymidine blocked in early S phase and released for the indicated times (lanes 1–4) or thymidine-nocodazole blocked in mitosis and released for the indicated times (lanes 5–8). Immunoblots measure the indicated protein abundance for BRCA1, NUSAP1, cyclin A, and cyclin B1 with matched loading controls, as indicated.

expression in the same samples. We synchronized HeLa cells at early S phase using a double thymidine block strategy. Similarly, we synchronized another set of cells in early mitosis using a thymidine–nocodazole sequential block. The former set of cells was released at the following different time-points: double thymidine block without release (0 h; early S phase); 3 h post-release (mid-S phase); 6 h post-release (late S phase/early G<sub>2</sub>); and 9 h post-release (G<sub>2</sub> phase). The second set of cells was released at the following time-points: nocodazole block without release (0 h, mitosis); 3 h post-release (early G<sub>1</sub> phase); 6 h post-release (G<sub>1</sub> phase); and 9 h post-release (late G<sub>1</sub> phase). Cell lysates were examined by immunoblotting for NUSAP1 and BRCA1 and compared with cyclin A and cyclin B1 (Fig. 3). BRCA1 protein

was abundant in extracts starting in early S phase and decreased to low levels after mitosis. Relative to BRCA1, NUSAP1 was slightly shifted in its expression, with protein abundant from late S through about 3 h into G<sub>1</sub>. Thus, BRCA1 and NUSAP1 were both abundant in cells during G<sub>2</sub>.

#### BRCA1 overexpression suppresses defects caused by NUSAP1 depletion in homologous recombination and centrosome duplication

NUSAP1 depletion disrupted the processes of homologous recombination and centrosome duplication. Since BRCA1 is important for both these processes, we tested whether BRCA1 depletion or overexpression could affect the phenotype of NUSAP1 depletion. When depleting BRCA1 together with NUSAP1, the phenotype of the HDR assay or centrosome assay was the same as when only BRCA1 was depleted (data not shown). By contrast, overexpression of BRCA1 in the same cells transfected with the NUSAP1-specific siRNA resulted in a partial reversal of the effects of NUSAP1 depletion. NUSAP1 depletion with add-back of empty vector decreased homologous recombination levels 2-fold (Fig. 4A), consistent with results in Figure 1. NUSAP1 depletion along with co-transfection of a plasmid expressing BRCA1 restored homologous recombination levels to 85% of full activity. Though NUSAP1 stabilized BRCA1, we did not detect co-immunoprecipitation of NUSAP1 and BRCA1 (data not shown); thus, we could not infer a direct interaction between these two factors.

We also performed concurrent NUSAP1 depletion and BRCA1 overexpression in the centrosome assay. Hs578T cells were co-transfected with NUSAP1 siRNA, plasmid for expressing BRCA1, and plasmid encoding GFP-centrin. Forty-eight hours post-transfection, cells were fixed and viewed by immunofluorescence. While NUSAP1 depletion with empty vector resulted in the formation of supernumerary centrosomes in 26% of cells (Fig. 4B), NUSAP1 depletion in conjunction with transfection of the BRCA1 expression plasmid resulted in a reduced percentage of cells with centrosome amplification to 10%, as compared with the control of 5% in this experiment.

Based on the previous result, we tested whether NUSAP1 depletion affected *BRCA1* mRNA levels, either directly or indirectly. We performed a quantitative real-time PCR analysis of RNA from transfected cells. HeLa cells were depleted of NUSAP1, and 48 h post-transfection total RNA was harvested from the cells and reverse transcribed into DNA. Real-time PCR of the resultant cDNAs were conducted using probes targeting the coding sequences of *BRCA1* and *NUSAP1* and normalized to the transcript levels of *RPS14*. It was found that BRCA1 and NUSAP1 depletions resulted in downregulation of the respective mRNAs, but siRNA specific to NUSAP1 did not affect *BRCA1* mRNA levels, nor did BRCA1 siRNA affect *NUSAP1* mRNA levels (Fig. 5A). Thus, NUSAP1 siRNA specifically targets *NUSAP1* mRNA and has no effect on *BRCA1* mRNA abundance.

We tested whether depletion of NUSAP1 affected BRCA1 protein levels in synchronized cells. Cells were synchronized in early S phase, using a double thymidine block and harvested at multiple time-points after thymidine release. Protein extracts were analyzed by immunoblotting. The different time-points—0, 3,

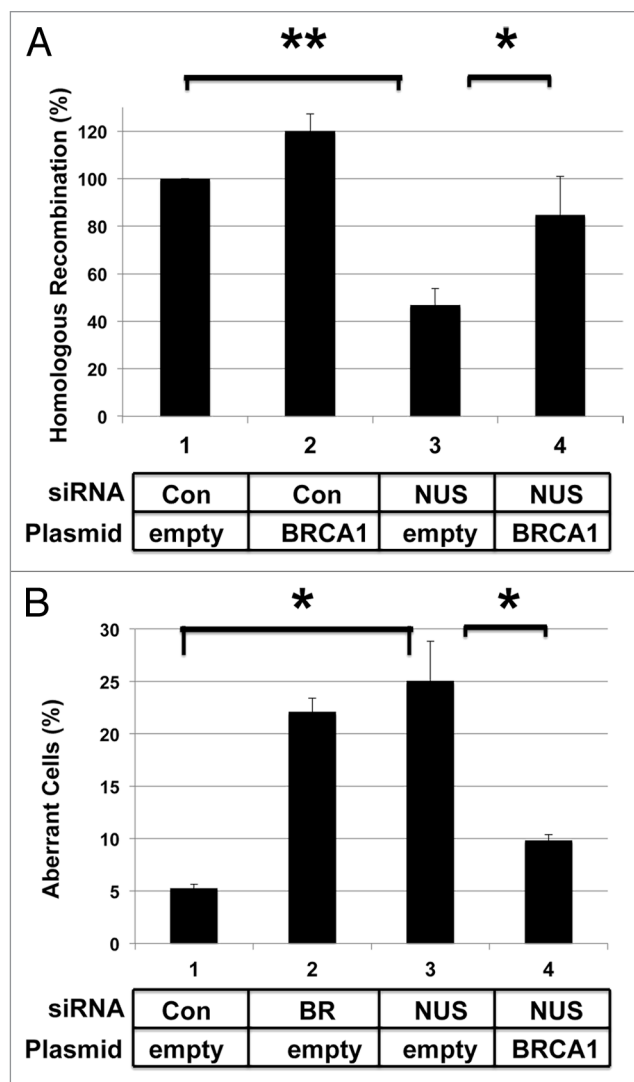


**Figure 4.** Expression of BRCA1 from a plasmid suppresses effects of NUSAP1 depletion. **(A)** HeLa-DR cells were transfected with the indicated siRNAs and a plasmid for the expression of BRCA1 (lanes 2 and 4). Results were obtained in triplicate and normalized relative to the control siRNA. A two-tailed Student *t* test compared the effects of NUSAP1 si-2 to the control siRNA (lane 3 vs. lane 1;  $P = 0.001603$ ) and the effect of rescue with BRCA1-expressing plasmid (lane 4 vs. lane 3;  $P = 0.04048$ ). **(B)** Hs578T cells were transfected with the indicated siRNAs and plasmids, along with an expression plasmid for GFP-centrin2, and the percentage of cells with supernumerary centrosomes is indicated. Results were obtained in triplicate plus SEM. A two-tailed Student *t* test compared the effects of NUSAP1 si-2 to the control siRNA (lane 3 vs. lane 1;  $P = 0.04099$ ) and the effect of rescue with BRCA1-expressing plasmid (lane 4 vs. lane 3;  $P = 0.04859$ ).

6, and 9 h post thymidine release—correspond to early S phase, mid S phase, late S phase, and  $G_2$  phase respectively. NUSAP1 depletion resulted in a decrease of BRCA1 protein levels at all the time-points (Fig. 5B). It was surprising that even during early S phase NUSAP1 depletion affected BRCA1 protein levels (lanes 1–3) since NUSAP1 is more abundant at later stages of the cell cycle (Fig. 3). Evidently, even the low concentration of NUSAP1 present in early S phase affects BRCA1 protein abundance.

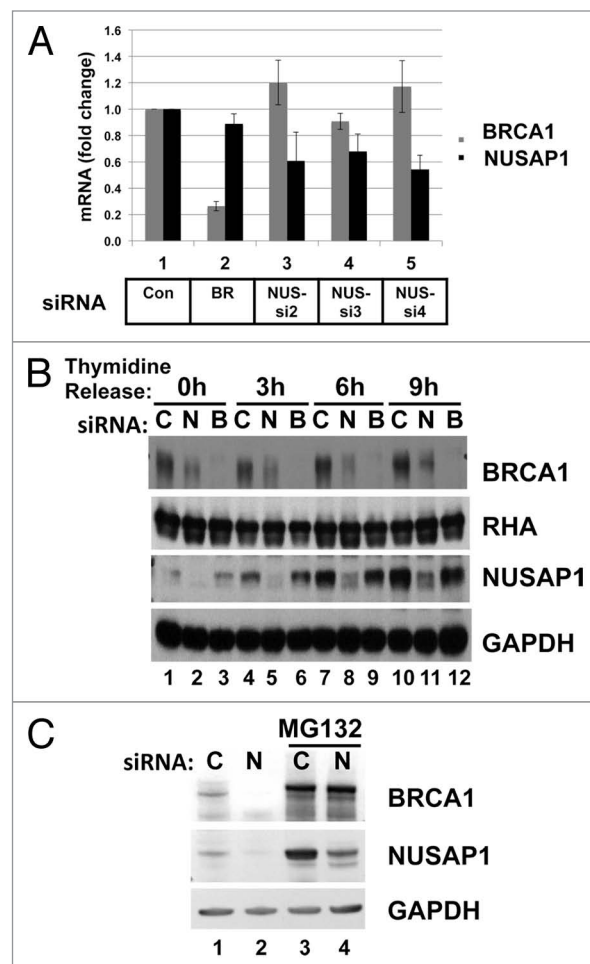


**Figure 5.** Depletion of NUSAP1 affects BRCA1 protein but not mRNA levels. **(A)** Two days following transfection of HeLa cells with the indicated siRNA, RNA was isolated and quantified by qPCR. Results, in triplicate, from BRCA1-specific primers are indicated in gray, and results from NUSAP1-specific primers are indicated in black. Results were normalized to the cells transfected with the control siRNA and presented with the standard error of the mean. **(B)** Cells were transfected with control (C; lanes 1, 4, 7, 10), NUSAP1 (N; lanes 2, 5, 8, 11), and BRCA1 (B; lanes 3, 6, 9, 12) specific siRNAs. Following double thymidine block and release for the indicated times, cell lysates were prepared and analyzed with the indicated immunoblots. RHA and GAPDH were loading controls. **(C)** Cells were transfected with control siRNA (C; lanes 1, 3) or NUSAP1 siRNA2 (N; lanes 2, 4) and subjected to a double thymidine block as in panel B. Two hours after thymidine release, 20  $\mu$ M MG132 was included in media for another 4 h (lanes 3, 4); DMSO vehicle was included in media at the same time in lanes 1 and 2.

Since BRCA1 is degraded by the proteasome,<sup>49</sup> we tested whether the NUSAP1-dependent stabilization of BRCA1 in late S phase also involved the proteasome. Following two siRNA transfections, cells were double blocked in thymidine and released for 6 h. The last 4 h of the release were in the presence of the proteasome inhibitor MG132 or the solvent control. As was observed in Figure 5B, depletion of NUSAP1 caused a decrease in BRCA1 protein content during late S phase (Fig. 5C, lanes 1 and 2). In the presence of MG132, BRCA1 protein was at increased concentration in the cell; interestingly NUSAP1 levels were markedly

higher as well (Fig. 5C, lane 3). Depletion of NUSAP1 reduced the level of NUSAP1, but it had no effect on the BRCA1 levels (Fig. 5C, lane 4). We thus interpret that NUSAP1 protects BRCA1 from proteasome-mediated degradation.

#### NUSAP1 depletion affects recruitment of BRCA1 to DNA damage foci

Our results so far are consistent with NUSAP1 impacting the homologous recombination process via controlling BRCA1 protein levels. We tested whether recruitment of BRCA1 to foci induced upon DNA damage<sup>7</sup> would also be affected by NUSAP1 depletion. Cells were irradiated and then stained for BRCA1 at 0 h or 6 h post-irradiation. Without irradiation, both control and NUSAP1 depleted cells had some discrete BRCA1 S-phase foci<sup>8,50</sup> plus diffusely nuclear BRCA1 content (Fig. 6A, top). However, 6 h post-irradiation, most of the control cells had irradiation-induced foci (IRIF) containing BRCA1, but few NUSAP1 depleted cells had detectable BRCA1 foci (Fig. 6A, bottom). There were cells with BRCA1-containing foci detected, but they were pale with low levels of BRCA1. We repeated the same experiment with NUSAP1 depletion, but with additional transfection of a vector expressing BRCA1, and this add-back restored the BRCA1 IRIF (data not shown).

We then analyzed other proteins in IRIF subsequent to NUSAP1 depletion. There was no difference in the levels of  $\gamma$ -H2AX IRIF between the control and NUSAP1 depleted cells (Fig. 6C). Western blot analysis also showed that  $\gamma$ -H2AX protein levels were not affected by NUSAP1 depletion upon irradiation (Fig. 6D). The phosphorylation of H2AX is an early sensor protein at the site of the double strand break upon DNA damage.<sup>51</sup> BRCA1 is downstream of  $\gamma$ -H2AX in the DNA damage response pathway,<sup>7</sup> and is required for assembly of RAD51 at IRIF, following DNA damage.<sup>52</sup> We thus tested whether RAD51 binding to IRIF was affected by NUSAP1 depletion. Depletion of NUSAP1 diminished, but did not eliminate, RAD51 recruitment to the IRIF (Fig. 6E). While there was no change in the percentage of cells expressing RAD51 foci, the intensity of the RAD51 foci was decreased when compared with those of the control cells. In a similar manner, we tested 53BP1 levels at IRIF upon NUSAP1 depletion. We observed that NUSAP1 depletion caused no reduction in 53BP1 recruitment to double strand breaks and were perhaps even more prominent than in control cells (Fig. 6G). Western analysis did not show any changes in 53BP1 protein levels in NUSAP1 depleted cells vs. control cells (Fig. 6H). This result suggested that NUSAP1 depletion affected the pathway regulated by BRCA1, but had no impact on the pathway regulated by 53BP1.

## Discussion

In this study, we have identified NUSAP1 as a potential modifier of BRCA1 function and found that, similar to BRCA1, NUSAP1 regulates the DNA repair by homologous recombination and control of centrosome number. NUSAP1 was first flagged for follow-up via gene coexpression analysis with *BRCA1*, *BRCA2*, and *BARD1* from multiple publicly available breast cancer microarray data sets and using multiple computational methods. In another study, we found that NUSAP1 is a component of a 412 gene/

protein network that regulates the cell cycle and DNA repair.<sup>35</sup> In this study, we found: (1) like BRCA1, NUSAP1 is required for high level of DSB repair by homologous recombination and by the minor pathway of repair by single-strand annealing; (2) NUSAP1 regulates centrosome number per cell; (3) surprisingly, we found that overexpression of BRCA1 suppressed the defect due to depletion of NUSAP1 in both DNA repair and in centrosome control; (4) NUSAP1 protected BRCA1 protein from proteasome-mediated degradation during S phase of the cell cycle; (5) the expression of NUSAP1 affected localization of BRCA1 to DNA repair foci; and (6) the requirement for NUSAP1 affected the binding of the downstream repair factor RAD51 to DNA repair foci.

Our results suggest that NUSAP1 functions via regulating BRCA1 protein levels from early S phase through G<sub>2</sub> phase. Since the evidence suggests that the NUSAP1 effect on homologous recombination is indirect via regulating BRCA1 levels, this would be consistent with NUSAP1 depletion having a lesser impact on homologous recombination compared with the BRCA1 depletion. Future work is aimed at understanding the mechanism by which the NUSAP1 protein affects the BRCA1 protein concentration. Further work will determine whether NUSAP1 has activities independent of BRCA1 stabilization in the DNA damage response.

This study is the first to link NUSAP1 with homologous recombination. Other studies have shown that NUSAP1 is phosphorylated by ATM/ATR kinases, and also gets degraded in response to UV damage.<sup>17-19</sup> NUSAP1 has been found to be involved in mitotic spindle assembly, and chromosome segregation.<sup>15</sup> These previously observed functions of NUSAP1 are consistent with our new observations that it has a role in homologous recombination and control of centrosome duplication.

Future studies on NUSAP1 will be focused on whether it is a genetic modifier of BRCA1 activity or whether it is itself a breast cancer associated gene. Among the large scale sequencing efforts of tumor samples in The Cancer Genome Atlas (TCGA), the *NUSAP1* gene is altered in 1–4% of the cases. Since our focus has been on BRCA1 and breast cancer, we note that a small percentage of breast tumors (<1% each) had homozygous deletions, amplifications, or missense mutations.<sup>53</sup> Other tumor types had a greater percentage of genetic abnormalities of the *NUSAP1* gene. About 3% each of cervical carcinoma, lung adenoma, and ovarian serous carcinoma had evidence of homozygous deletions of the *NUSAP1* gene.<sup>54,55</sup> Though a small percentage of the overall cancers, deletion of *NUSAP1* can contribute to the phenotype of these cancers. According to the results of the current study, deletion of *NUSAP1* would decrease BRCA1 protein levels. Since BRCA1 has been implicated in ovarian cancer, it is reasonable that NUSAP1 control of BRCA1 protein levels could contribute to ovarian tumorigenesis. A similar mechanism for NUSAP1 might apply to other cancer types, such as cervical carcinoma and lung adenoma, which have deletions of the gene.

## Materials and Methods

### Cell culture and reagents

The HeLa-DR, SA-GFP, and Hs578T cell lines have been described previously.<sup>39-42</sup> The siRNA sequences for BRCA1 and

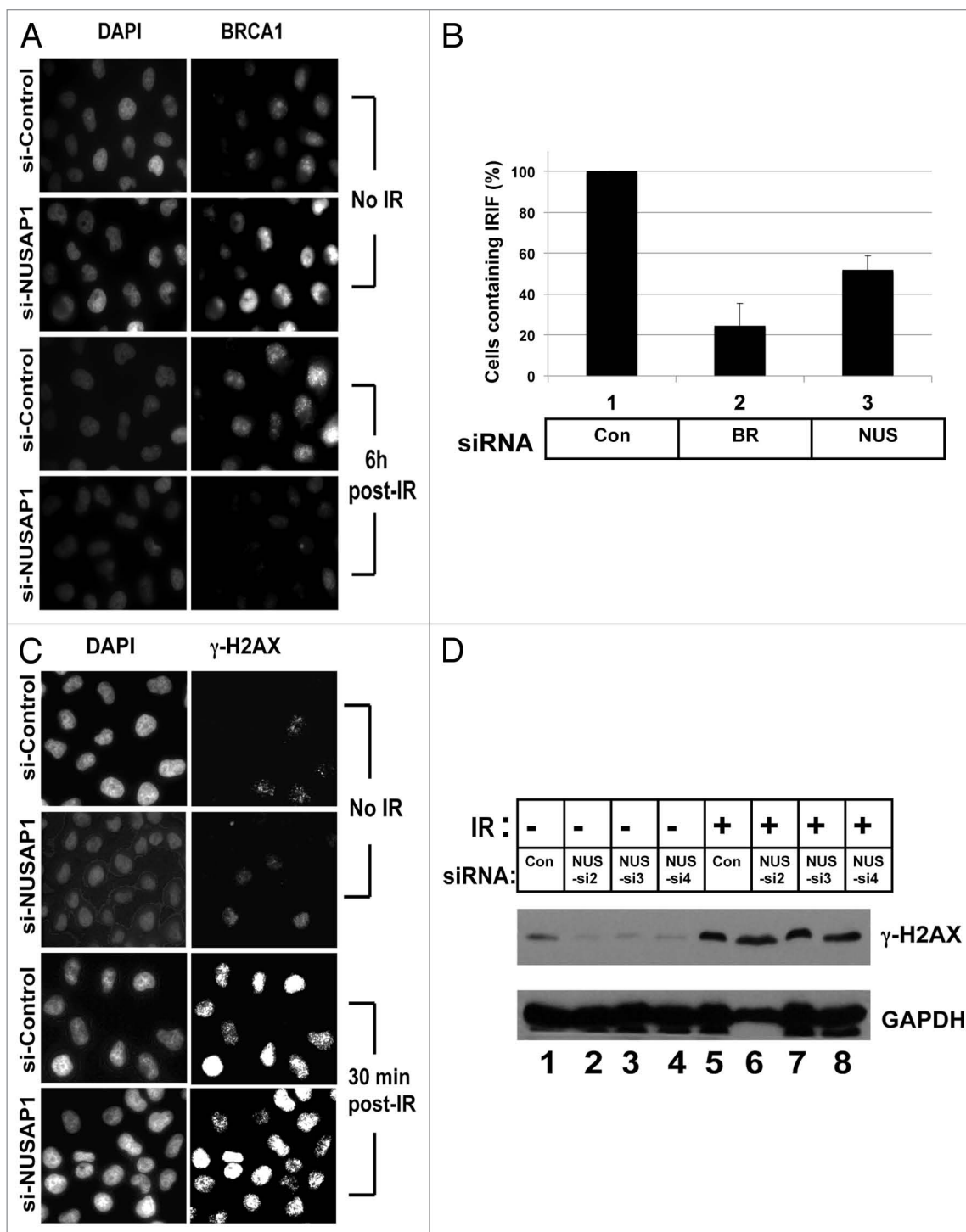
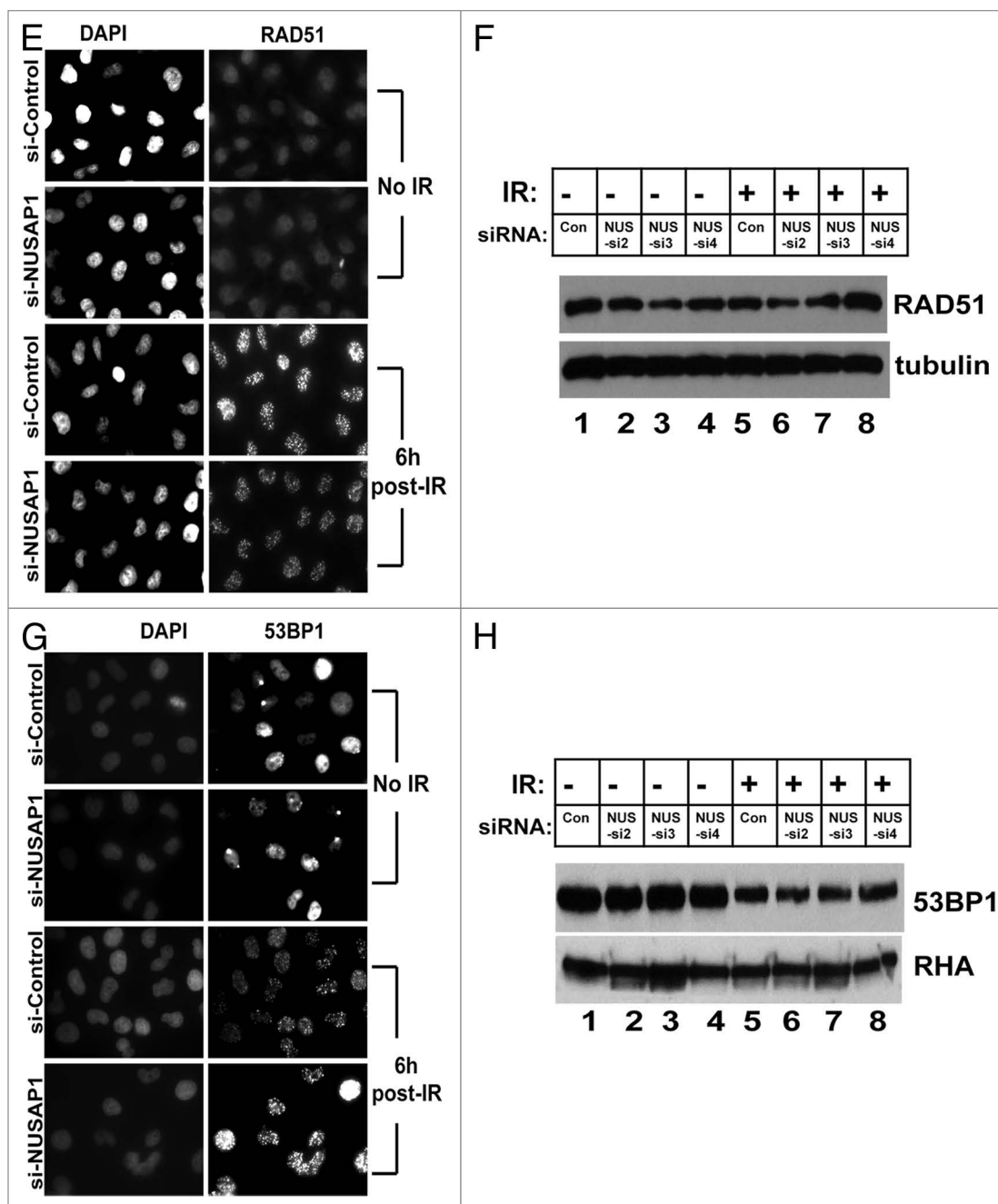


**Figure 6A–D** (For E–H, see page 540). NUSAP1 depletion affects BRCA1 and RAD51 localization to DNA damage induced foci. **(A)** HeLa cells were transfected with control or NUSAP1 specific siRNAs and stained for DNA content (left) or BRCA1 content (right) before (top) or after (bottom) 10 Gy of ionizing radiation. **(B)** The number of cells with detectable BRCA1 IRIF from **(A)** is indicated, normalized relative to the control siRNA plus the SEM **(C)** Cells transfected as in panel A were stained for  $\gamma$ -H2AX, as indicated. **(D)** Cell lysates were prepared from the transfected cells in **(C)** and immunoblots were probed with antibody specific to  $\gamma$ -H2AX, and GAPDH is the loading control.

NUSAP1 are listed in Table S1. Antibodies for BRCA1 (sc-642), RAD51 (H-92), and 53BP1 (H-300) were procured from Santa Cruz Biotechnology, and  $\gamma$ -H2AX (ser 139,

JBW301) and BRCA1 (OP-92) from EMD-Millipore. The antibody for NUSAP1 was prepared by immunizing rabbits with full-length NUSAP1 protein purified from bacterial; immunization



of rabbits and harvesting of sera was performed by Cocalico Biologicals. Secondary antibodies Alexa Fluor 488 and Alexa Fluor 568 were purchased from Invitrogen.

#### Transfection

On day 1, we seed cells ( $\sim 2 \times 10^5$  in a 10-cm<sup>2</sup> well) such that they are 50% confluent on day 2. On day 2, 60 pmoles of siRNA with 0.8  $\mu$ g plasmid were transfected into the cells using 0.5  $\mu$ L lipofectamine (Invitrogen). On day 4, 100 pmoles of siRNA with 3  $\mu$ g of plasmid were transfected in using 2.5  $\mu$ L

lipofectamine (Invitrogen). Optimem was used as the dilution medium, and transfection medium was always changed 6 h post transfection.

#### Western analysis

Cell lysates were harvested using a lysis buffer containing the following: 50 mM TRIS, 300 mM NaCl, 0.5% NP40, 1 mM EDTA, 5% glycerol. Alternately, lysates were also prepared using a SDS lysis buffer containing the following: 50 mM TRIS pH 6.8, 2% SDS, 10% glycerol, 5%  $\beta$ -mercaptoethanol, and

0.25% bromophenol blue dye to color. Cell lysates were centrifuged at 15 000 rpm for 20 min, and supernatants were collected. Protein concentration of the supernatant was analyzed using Bio-Rad Bradford reagent. Fifty micrograms protein lysates were analyzed by SDS-PAGE and transferred to polyvinylidene fluoride membranes and immunoblotted using standard methods.

#### Homology-directed repair assay

The homologous recombination using the HeLa-DR cell line was done as previously described.<sup>40,56</sup> GFP-positive cells, indicative of recombination events, were scored by flow cytometry using a BD Biosciences FACS Calibur instrument located at the Ohio State Comprehensive Cancer Center (OSUCCC) Analytical Flow Cytometry core laboratory.

#### Single strand annealing assay

The SA-GFP recombinant cell line was created using stable integration of an hpRT-SA-GFP vector<sup>41</sup> into HeLa cells. On day 1, SA-GFP cells were plated at a cell density of  $4 \times 10^4$  cells in a 2 cm<sup>2</sup> well. On day 2, the first transfection was performed on cells that were 50% confluent, using 60 pmol of siRNA and 1.5  $\mu$ L of Oligofectamine in Optimem. The cells were transferred to 10 cm<sup>2</sup> dishes on day 3. On day 4, transfection was performed using 100 pmol of siRNA, 2.5  $\mu$ L of Lipofectamine, and 3  $\mu$ g of pCBASceI plasmid. We analyzed the cells for green fluorescence by FACS analysis.

#### Centrosome duplication assay

This assay was performed in Hs578T cells using an established technique.<sup>53</sup> NUSAP1 siRNA and a pJLS148-GFP-centrin vector<sup>46</sup> were simultaneously transfected using Lipofectamine 2000. 48 h post-transfection, cells were washed with phosphate buffered saline (PBS), fixed with methanol (at -20 °C), washed with PBS again, and then treated with DAPI (4',6-diamidino-2-phenylindole). Over 100 cells per experiment were analyzed in three replicate experiments, using a Zeiss Axiovert 200 M immunofluorescence microscope, for the number of centrioles per cell, which are labeled by the GFP-centrin vector.

#### RNA extraction and reverse transcription

HeLa cells were depleted of BRCA1 and NUSAP1 using RNAi as described above. Forty-eight hours post-transfection, total RNA was extracted and purified from the cells using

Trizol reagent (Invitrogen). RNA samples were quantified using Nanodrop ND-1000 Spectrophotometer, and 1  $\mu$ g/sample of RNA template was reverse transcribed using the iScript cDNA Synthesis kit (Bio-Rad).

#### Quantitative real-time PCR (Q-PCR) analysis

The primers used are listed in Table S2. *RPS14* was used as the endogenous control and samples treated with control siRNA acted as the reference. SYBR Green was used as the fluorescent dye using the iQ SYBR Green Supermix kit (Bio-Rad) in the Applied Biosystems StepOne Plus Real-Time PCR System. Samples were run in duplicate and standard deviation was calculated. Results were calculated using the  $2^{-\Delta\Delta C_t}$  formula.

#### Immunocytochemistry

Cells were washed with PBS and fixed with 4% paraformaldehyde in PBS. Next, cells were permeabilized using 0.25% Triton-X-100 in PBS, and blocked in buffer containing 1% goat serum. Cells were then probed using specific primary antibodies, followed by Alexa Fluor secondary antibodies in buffer containing 0.1% BSA and 6% Triton X-100. Lastly, cells were stained with DAPI, and then treated with Prolong Gold anti-fade reagent (Invitrogen). Cells were viewed using the Zeiss Axiovert 200 M microscope.

#### Statistical analyses

Comparison of treatments with the controls was done utilizing a pairwise Student *t* test. Figures were labeled with \**P* < 0.05, \*\**P* < 0.01, and \*\*\**P* < 0.001.

#### Disclosure of Potential Conflicts of Interest

No potential conflicts of interest were disclosed.

#### Acknowledgments

We are grateful to Dr J Stark of the Beckman Research Institute of the City of Hope for the kind gift of recombination substrates used in this study. This work was supported by NIH grant R01 CA141090 to K.H., U.V.C., and J.D.P.

#### Supplemental Materials

Supplemental materials may be found here: [www.landesbioscience.com/journals/cbt/article/28019](http://www.landesbioscience.com/journals/cbt/article/28019)

#### References

- Huen MS, Sy SM, Chen J. BRCA1 and its toolbox for the maintenance of genome integrity. *Nat Rev Mol Cell Biol* 2010; 11:138-48; PMID:20029420; <http://dx.doi.org/10.1038/nrm2831>
- Miki Y, Swensen J, Shattuck-Eidens D, Futreal PA, Harshman K, Tavtigian S, Liu Q, Cochran C, Bennett LM, Ding W, et al. A strong candidate for the breast and ovarian cancer susceptibility gene BRCA1. *Science* 1994; 266:66-71; PMID:7545954; <http://dx.doi.org/10.1126/science.7545954>
- Xu B, O'Donnell AH, Kim ST, Kastan MB. Phosphorylation of serine 1387 in Brca1 is specifically required for the Atm-mediated S-phase checkpoint after ionizing irradiation. *Cancer Res* 2002; 62:4588-91; PMID:12183412
- Kim H, Huang J, Chen J. CCDC98 is a BRCA1-BRCT domain-binding protein involved in the DNA damage response. *Nat Struct Mol Biol* 2007; 14:710-5; PMID:17643122; <http://dx.doi.org/10.1038/nsmb1277>
- Starita LM, Parvin JD. The multiple nuclear functions of BRCA1: transcription, ubiquitination and DNA repair. *Curr Opin Cell Biol* 2003; 15:345-50; PMID:12787778; [http://dx.doi.org/10.1016/S0955-0674\(03\)00042-5](http://dx.doi.org/10.1016/S0955-0674(03)00042-5)
- Wang B, Matsuo S, Ballif BA, Zhang D, Smogorzewska A, Gygi SP, Elledge SJ. Abraxas and RAP80 form a BRCA1 protein complex required for the DNA damage response. *Science* 2007; 316:1194-8; PMID:17525340; <http://dx.doi.org/10.1126/science.1139476>
- Paull TT, Rogakou EP, Yamazaki V, Kirchgessner CU, Gellert M, Bonner WM. A critical role for histone H2AX in recruitment of repair factors to nuclear foci after DNA damage. *Curr Biol* 2000; 10:886-95; PMID:10959836; [http://dx.doi.org/10.1016/S0960-9822\(00\)00610-2](http://dx.doi.org/10.1016/S0960-9822(00)00610-2)
- Scully R, Chen J, Plug A, Xiao Y, Weaver D, Feunteun J, Ashley T, Livingston DM. Association of BRCA1 with Rad51 in mitotic and meiotic cells. *Cell* 1997; 88:265-75; PMID:9008167; [http://dx.doi.org/10.1016/S0092-8674\(00\)81847-4](http://dx.doi.org/10.1016/S0092-8674(00)81847-4)
- Moynahan ME, Chiu JW, Koller BH, Jasin M. Brca1 controls homology-directed DNA repair. *Mol Cell* 1999; 4:511-8; PMID:10549283; [http://dx.doi.org/10.1016/S1097-2765\(00\)80202-6](http://dx.doi.org/10.1016/S1097-2765(00)80202-6)
- Snouwaert JN, Gowen LC, Latour AM, Mohn AR, Xiao A, DiBiase L, Koller BH. BRCA1 deficient embryonic stem cells display a decreased homologous recombination frequency and an increased frequency of non-homologous recombination that is corrected by expression of a brca1 transgene. *Oncogene* 1999; 18:7900-7; PMID:10630642; <http://dx.doi.org/10.1038/sj.onc.1203334>
- Stark JM, Pierce AJ, Oh J, Pastink A, Jasin M. Genetic steps of mammalian homologous repair with distinct mutagenic consequences. *Mol Cell Biol* 2004; 24:9305-16; PMID:15485900; <http://dx.doi.org/10.1128/MCB.24.21.9305-9316.2004>
- Zhong Q, Boyer TG, Chen PL, Lee WH. Deficient nonhomologous end-joining activity in cell-free extracts from Brca1-null fibroblasts. *Cancer Res* 2002; 62:3966-70; PMID:12124328

13. Harper JW, Elledge SJ. The DNA damage response: ten years after. *Mol Cell* 2007; 28:739-45; PMID:18082599; <http://dx.doi.org/10.1016/j.molcel.2007.11.015>
14. Huen MS, Chen J. The DNA damage response pathways: at the crossroad of protein modifications. *Cell Res* 2008; 18:8-16; PMID:18087291; <http://dx.doi.org/10.1038/cr.2007.109>
15. Raemaekers T, Ribbeck K, Beaudouin J, Annaert W, Van Camp M, Stockmans I, Smets N, Bouillon R, Ellenberg J, Carmeliet G. NuSAP, a novel microtubule-associated protein involved in mitotic spindle organization. *J Cell Biol* 2003; 162:1017-29; PMID:12963707; <http://dx.doi.org/10.1083/jcb.200302129>
16. Vanden Bosch A, Raemaekers T, Denayer S, Torrekens S, Smets N, Moermans K, Dewerchin M, Carmeliet P, Carmeliet G. NuSAP is essential for chromatin-induced spindle formation during early embryogenesis. *J Cell Sci* 2010; 123:3244-55; PMID:20807801; <http://dx.doi.org/10.1242/jcs.063875>
17. Matsuoka S, Ballif BA, Smogorzewska A, McDonald ER 3<sup>rd</sup>, Hurov KE, Luo J, Bakalarski CE, Zhao Z, Solimini N, Lerenthal Y, et al. ATM and ATR substrate analysis reveals extensive protein networks responsive to DNA damage. *Science* 2007; 316:1160-6; PMID:17525332; <http://dx.doi.org/10.1126/science.1140321>
18. Xie P, Li L, Xing G, Tian C, Yin Y, He F, Zhang L. ATM-mediated NuSAP phosphorylation induces mitotic arrest. *Biochem Biophys Res Commun* 2011; 404:413-8; PMID:21130744; <http://dx.doi.org/10.1016/j.bbrc.2010.11.135>
19. Emanuele MJ, Elia AE, Xu Q, Thoma CR, Izhar L, Leng Y, Guo A, Chen YN, Rush J, Hsu PW, et al. Global identification of modular cullin-RING ligase substrates. *Cell* 2011; 147:459-74; PMID:21963094; <http://dx.doi.org/10.1016/j.cell.2011.09.019>
20. Bogunovic D, O'Neill DW, Belitskaya-Levy I, Vacic V, Yu YL, Adams S, Darvishian F, Berman R, Shapiro R, Pavlick AC, et al. Immune profile and mitotic index of metastatic melanoma lesions enhance clinical staging in predicting patient survival. *Proc Natl Acad Sci U S A* 2009; 106:20429-34; PMID:19915147; <http://dx.doi.org/10.1073/pnas.0905139106>
21. Gulzar ZG, McKenney JK, Brooks JD. Increased expression of NuSAP in recurrent prostate cancer is mediated by E2F1. *Oncogene* 2013; 32:70-7; PMID:22349817; <http://dx.doi.org/10.1038/onc.2012.27>
22. Marie SK, Okamoto OK, Uno M, Hasegawa AP, Oba-Shinjo SM, Cohen T, Camargo AA, Kosoy A, Carlotti CG Jr., Toledo S, et al. Maternal embryonic leucine zipper kinase transcript abundance correlates with malignancy grade in human astrocytomas. *Int J Cancer* 2008; 122:807-15; PMID:17960622; <http://dx.doi.org/10.1002/ijc.23189>
23. Ryu B, Kim DS, Deluca AM, Alani RM. Comprehensive expression profiling of tumor cell lines identifies molecular signatures of melanoma progression. *PLoS One* 2007; 2:e594; PMID:17611626; <http://dx.doi.org/10.1371/journal.pone.0000594>
24. Satow R, Shitashige M, Kanai Y, Takeshita F, Ojima H, Jigami T, Honda K, Kosuge T, Ochiya T, Hirohashi S, et al. Combined functional genome survey of therapeutic targets for hepatocellular carcinoma. *Clin Cancer Res* 2010; 16:2518-28; PMID:20388846; <http://dx.doi.org/10.1158/1078-0432.CCR-09-2214>
25. Wadia PP, Coram M, Armstrong RJ, Mindrinos M, Butte AJ, Miklos DB. Antibodies specifically target AML antigen NuSAP1 after allogeneic bone marrow transplantation. *Blood* 2010; 115:2077-87; PMID:20053754; <http://dx.doi.org/10.1182/blood-2009-03-211375>
26. Chen DT, Nasir A, Culhane A, Venkataramu C, Fulp W, Rubio R, Wang T, Agrawal D, McCarthy SM, Gruidl M, et al. Proliferative genes dominate malignancy-risk gene signature in histologically-normal breast tissue. *Breast Cancer Res Treat* 2010; 119:335-46; PMID:19266279; <http://dx.doi.org/10.1007/s10549-009-0344-y>
27. Kokkinakis DM, Liu X, Neuner RD. Modulation of cell cycle and gene expression in pancreatic tumor cell lines by methionine deprivation (methionine stress): implications to the therapy of pancreatic adenocarcinoma. *Mol Cancer Ther* 2005; 4:1338-48; PMID:16170025; <http://dx.doi.org/10.1158/1535-7163.MCT-05-0141>
28. Lauss M, Kriegner A, Vierlinger K, Visne I, Yildiz A, Dilaveroglu E, Noehammer C. Consensus genes of the literature to predict breast cancer recurrence. *Breast Cancer Res Treat* 2008; 110:235-44; PMID:17899371; <http://dx.doi.org/10.1007/s10549-007-9716-3>
29. Stuart JE, Lusis EA, Scheck AC, Coons SW, Lal A, Perry A, Gutmann DH. Identification of gene markers associated with aggressive meningioma by filtering across multiple sets of gene expression arrays. *J Neuropathol Exp Neurol* 2011; 70:1-12; PMID:21157382; <http://dx.doi.org/10.1097/NEN.0b013e3182018f1c>
30. Kretschmer C, Sterner-Kock A, Siedentopf F, Schoenegg W, Schlag PM, Kemmer W. Identification of early molecular markers for breast cancer. *Mol Cancer* 2011; 10:15; PMID:21314937; <http://dx.doi.org/10.1186/1476-4598-10-15>
31. Cario G, Fetz A, Bretscher C, Möricke A, Schrauder A, Stanulla M, Schrappe M. Initial leukemic gene expression profiles of patients with poor in vivo prednisone response are similar to those of blasts persisting under prednisone treatment in childhood acute lymphoblastic leukemia. *Ann Hematol* 2008; 87:709-16; PMID:18521602; <http://dx.doi.org/10.1007/s00277-008-0504-x>
32. Ghousaini M, Fletcher O, Michailidou K, Turnbull C, Schmidt MK, Dicks E, Dennis J, Wang Q, Humphreys MK, Luccarini C, et al.; Netherlands Collaborative Group on Hereditary Breast and Ovarian Cancer (HEBON); Familial Breast Cancer Study (FBCS); Gene Environment Interaction of Breast Cancer in Germany (GENICA) Network; kConFab Investigators; Australian Ovarian Cancer Study Group. Genome-wide association analysis identifies three new breast cancer susceptibility loci. *Nat Genet* 2012; 44:312-8; PMID:22267197; <http://dx.doi.org/10.1038/ng.1049>
33. Michailidou K, Hall P, Gonzalez-Neira A, Ghousaini M, Dennis J, Milne RL, Schmidt MK, Chang-Claude J, Bojesen SE, Bolla MK, et al.; Breast and Ovarian Cancer Susceptibility Collaboration; Hereditary Breast and Ovarian Cancer Research Group Netherlands (HEBON); kConFab Investigators; Australian Ovarian Cancer Study Group; GENICA (Gene Environment Interaction and Breast Cancer in Germany) Network. Large-scale genotyping identifies 41 new loci associated with breast cancer risk. *Nat Genet* 2013; 45:353-61, e1-2; PMID:23535729; <http://dx.doi.org/10.1038/ng.2563>
34. Pujana MA, Han JD, Starita LM, Stevens KN, Tewari M, Ahn JS, Rennett G, Moreno V, Kirchhoff T, Gold B, et al. Network modeling links breast cancer susceptibility and centrosome dysfunction. *Nat Genet* 2007; 39:1338-49; PMID:17922014; <http://dx.doi.org/10.1038/ng.2007.2>
35. Zhang J, Lu K, Xiang Y, Islam M, Kotian S, Kais Z, Lee C, Arora M, Liu HW, Parvin JD, et al. Weighted frequent gene co-expression network mining to identify genes involved in genome stability. *PLoS Comput Biol* 2012; 8:e1002656; PMID:22956898; <http://dx.doi.org/10.1371/journal.pcbi.1002656>
36. Kais Z, Barsky SH, Mathsyaraja H, Zha A, Ransburgh DJ, He G, Pilarski RT, Shapiro CL, Huang K, Parvin JD. KIAA0101 interacts with BRCA1 and regulates centrosome number. *Mol Cancer Res* 2011; 9:1091-9; PMID:21673012; <http://dx.doi.org/10.1158/1541-7786.MCR-10-0503>
37. Bozdag D, Parvin JD, Catalyurek UV. A Biclustering Method to Discover Co-regulated Genes Using Diverse Gene Expression Datasets. *Proceedings of First International Conference on Bioinformatics and Computational Biology (BICoB), LNCS* 2009; 5462:151-63.
38. Eren K, Deveci M, Küçükünç O, Çatalyürek UV. A comparative analysis of biclustering algorithms for gene expression data. *Brief Bioinform* 2013; 14:279-92; PMID:22772837; <http://dx.doi.org/10.1093/bib/bbs032>
39. Pierce AJ, Johnson RD, Thompson LH, Jasin M. XRCC3 promotes homology-directed repair of DNA damage in mammalian cells. *Genes Dev* 1999; 13:2633-8; PMID:10541549; <http://dx.doi.org/10.1101/gad.13.20.2633>
40. Ransburgh DJ, Chiba N, Ishioka C, Toland AE, Parvin JD. Identification of breast tumor mutations in BRCA1 that abolish its function in homologous DNA recombination. *Cancer Res* 2010; 70:988-95; PMID:20103620; <http://dx.doi.org/10.1158/0008-5472.CAN-09-2850>
41. Bennardo N, Cheng A, Huang N, Stark JM. Alternative-NHEJ is a mechanistically distinct pathway of mammalian chromosome break repair. *PLoS Genet* 2008; 4:e1000110; PMID:18584027; <http://dx.doi.org/10.1371/journal.pgen.1000110>
42. Towler WI, Zhang J, Ransburgh DJ, Toland AE, Ishioka C, Chiba N, Parvin JD. Analysis of BRCA1 variants in double-strand break repair by homologous recombination and single-strand annealing. *Hum Mutat* 2013; 34:439-45; PMID:23161852; <http://dx.doi.org/10.1002/humu.22251>
43. Starita LM, Machida Y, Sankaran S, Elias JE, Griffin K, Schlegel BP, Gygi SP, Parvin JD. BRCA1-dependent ubiquitination of gamma-tubulin regulates centrosome number. *Mol Cell Biol* 2004; 24:8457-66; PMID:15367667; <http://dx.doi.org/10.1128/MCB.24.19.8457-8466.2004>
44. Kais Z, Chiba N, Ishioka C, Parvin JD. Functional differences among BRCA1 missense mutations in the control of centrosome duplication. *Oncogene* 2012; 31:799-804; PMID:21725363; <http://dx.doi.org/10.1038/onc.2011.271>
45. Sankaran S, Starita LM, Groen AC, Ko MJ, Parvin JD. Centrosomal microtubule nucleation activity is inhibited by BRCA1-dependent ubiquitination. *Mol Cell Biol* 2005; 25:8656-68; PMID:16166645; <http://dx.doi.org/10.1128/MCB.25.19.8656-8668.2005>
46. Lingle WL, Salisbury JL. Methods for the analysis of centrosome reproduction in cancer cells. *Methods Cell Biol* 2001; 67:325-36; PMID:11550478; [http://dx.doi.org/10.1016/S0091-679X\(01\)67022-5](http://dx.doi.org/10.1016/S0091-679X(01)67022-5)
47. D'Assoro AB, Stivala F, Barrett S, Ferrigno G, Salisbury JL. GFP-centrin as a marker for centriole dynamics in the human breast cancer cell line MCF-7. *Ital J Anat Embryol* 2001; 106(Suppl 1):103-10; PMID:11729945
48. Ruffner H, Verma IM. BRCA1 is a cell cycle-regulated nuclear phosphoprotein. *Proc Natl Acad Sci U S A* 1997; 94:7138-43; PMID:9207057; <http://dx.doi.org/10.1073/pnas.94.14.7138>
49. Choudhury AD, Xu H, Baer R. Ubiquitination and proteasomal degradation of the BRCA1 tumor suppressor is regulated during cell cycle progression. *J Biol Chem* 2004; 279:33909-18; PMID:15166217; <http://dx.doi.org/10.1074/jbc.M403646200>

50. Jin Y, Xu XL, Yang MC, Wei F, Ayi TC, Bowcock AM, Baer R. Cell cycle-dependent colocalization of BARD1 and BRCA1 proteins in discrete nuclear domains. *Proc Natl Acad Sci U S A* 1997; 94:12075-80; PMID:9342365; <http://dx.doi.org/10.1073/pnas.94.22.12075>
51. Rogakou EP, Pilch DR, Orr AH, Ivanova VS, Bonner WM. DNA double-stranded breaks induce histone H2AX phosphorylation on serine 139. *J Biol Chem* 1998; 273:5858-68; PMID:9488723; <http://dx.doi.org/10.1074/jbc.273.10.5858>
52. Bhattacharyya A, Ear US, Koller BH, Weichselbaum RR, Bishop DK. The breast cancer susceptibility gene BRCA1 is required for subnuclear assembly of Rad51 and survival following treatment with the DNA cross-linking agent cisplatin. *J Biol Chem* 2000; 275:23899-903; PMID:10843985; <http://dx.doi.org/10.1074/jbc.C000276200>
53. Cancer Genome Atlas Network. Comprehensive molecular portraits of human breast tumours. *Nature* 2012; 490:61-70; PMID:23000897; <http://dx.doi.org/10.1038/nature11412>
54. Cerami E, Gao J, Dogrusoz U, Gross BE, Sumer SO, Aksoy BA, Jacobsen A, Byrne CJ, Heuer ML, Larsson E, et al. The cBio cancer genomics portal: an open platform for exploring multidimensional cancer genomics data. *Cancer Discov* 2012; 2:401-4; PMID:22588877; <http://dx.doi.org/10.1158/2159-8290.CD-12-0095>
55. Gao J, Aksoy BA, Dogrusoz U, Dresdner G, Gross B, Sumer SO, Sun Y, Jacobsen A, Sinha R, Larsson E, et al. Integrative analysis of complex cancer genomics and clinical profiles using the cBioPortal. *Sci Signal* 2013; 6:pl1; PMID:23550210; <http://dx.doi.org/10.1126/scisignal.2004088>
56. Kotian S, Liyanarachchi S, Zelent A, Parvin JD. Histone deacetylases 9 and 10 are required for homologous recombination. *J Biol Chem* 2011; 286:7722-6; PMID:21247901; <http://dx.doi.org/10.1074/jbc.C110.194233>